J. Biochem. **134**, 277–285 (2003)
DOI: 10.1093/jb/mvg141

Reaction of Aspartate Aminotransferase with C5-Dicarboxylic Acids: Comparison with the Reaction with C4-Dicarboxylic Acids

Mohammad Mainul Islam, Hideyuki Hayashi and Hiroyuki Kagamiyama*
Department of Biochemistry, Osaka Medical College, 2-7 Daigakumachi, Takatsuki 569-8686

Received April 23, 2003; accepted June 13, 2003

The reaction of *Escherichia coli* aspartate aminotransferase (AspAT) with glutamate and other C5-dicarboxylates was analyzed in order to compare its mechanism of action toward C5 substrates with that toward C4 substrates, which had been extensively characterized. The association of the amino-group protonated and unprotonated forms of glutamate (SH^+ and S, respectively) with the Schiff-base protonated and unprotonated forms of the enzyme (E_LH^+ and E_L, respectively) yields at least three forms of the Michaelis complex, whereas in the case of aspartate, only two species of this complex exist, $E_L{\cdot}SH^+$ and $E_LH^+{\cdot}S$. The reaction of AspAT with 2-methylglutamate can be explained only when we consider all the protonation states of the Michaelis complex. Based on the previous crystallographic studies [Miyahara *et al.* (1994) *J. Biochem.* 116, 1001–1012], we consider that glutamate binds to the open form of AspAT and takes an extended conformation in the Michaelis complex, with the α-amino group of glutamate oriented in the opposite direction to the Schiff base. This is in contrast to the Michaelis complex of aspartate, in which a strong interaction of the α-amino group of aspartate and the Schiff base excludes the presence of the species $E_LH^+{\cdot}SH^+$. It is concluded that AspAT recognizes the two types of dicarboxylates with different chain lengths by changing the gross conformation of the enzyme protein.

Key words: active site, aspartate-aminotransferase, conformation, kinetics, pyridoxal-5-phosphate, reaction-mechanism, substrate-recognition.

Abbreviations: AspAT, aspartate amino acid aminotransferase (aspartate:2-oxoglutarate aminotransferase, EC2.6.1.1); HEPES, 1-(2-hydroxyethyl)piperazine-4-(2-ethanesulfonic acid); K258A AspAT, AspAT in which Lys258 is mutated to alanine; MES, 4-morpholineethane-sulfonic acid; PIPES, 1,4-piperazine-bis(ethanesulfonic acid); PLP, pyridoxal 5′-phosphate; PMP, pyridoxamine 5′-phosphate; TAPS, 3-((tris(hydroxymethyl)methyl)amino)-1-propane-sulfonic acid; WT AspAT, wild-type AspAT.

Aspartate aminotransferase (AspAT; aspartate:2-oxoglutarate aminotransferase, EC2.6.1.1) is a pyridoxal 5′-phosphate (PLP)–dependent enzyme that catalyzes the reversible transamination between C4 (aspartate and oxalacetate) and C5 (glutamate and 2-oxoglutarate) dicarboxylic substrates by the following ping-pong Bi-Bi mechanism (*2*):

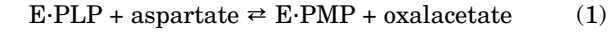

$$E{\cdot}PLP + \text{aspartate} \rightleftarrows E{\cdot}PMP + \text{oxalacetate} \quad (1)$$

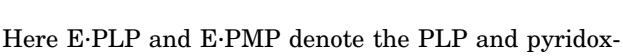

$$E{\cdot}PMP + \text{2-oxoglutarate} \rightleftarrows E{\cdot}PLP + \text{glutamate} \quad (2)$$

Here E·PLP and E·PMP denote the PLP and pyridoxamine 5′-phosphate (PMP) forms of the enzyme, respectively. Based on crystallographic studies of this enzyme (*3–9*), the mechanism of the first half-reaction (Eq. 1) has been studied (*10–15*) and proposed as follows (Scheme 1A). PLP forms a Schiff base with the ε-amino group of Lys258, and the imine N of the aldimine has a pK_a in the neutral region. The enzyme with an unprotonated Schiff base (E_L) reacts with aspartate with a protonated α-amino group (SH^+), and the enzyme with a protonated Schiff base (E_LH^+) reacts with aspartate with unprotonated α-amino group (S). Thus, the Michaelis complex (ES_1) comprises two species ($E_L{\cdot}SH^+$ and $E_LH^+{\cdot}S$), which interconvert rapidly. The species $E_LH^+{\cdot}S$ undergoes transaldimination to yield the enzyme–substrate complex in which PLP forms a Schiff base with the α-amino group of aspartate. In this complex (ES_2), called the external aldimine, a proton is shared by the imine N and the ε-amino group of Lys258, which is liberated from PLP through transaldimination. Therefore, similarly to the Michaelis complex, the external aldimine is a mixture of two species, $E_LH^+{=}S$ and $H^+E_L{=}S$, which are supposed to interconvert rapidly. The free ε-amino group of Lys258 in $E_LH^+{=}S$ abstracts the α-proton of aspartate, and transfers it to C4′ of PLP to form the ketimine (ES_4). The ketimine is hydrolyzed to form oxalacetate (P) and the PMP-form of the enzyme (E_M) by the catalysis of the Lys258 ε-amino group. One of the characteristics of this reaction pathway is that both the Michaelis complex and the external aldimine are mixtures of two species that have the same number of protons but differ in the position of protonation, and the species with the protonated Schiff base is the active species advancing to the next step. The pK_a of the Schiff base is elevated in these intermediates to accelerate catalysis (*14*, *16*). The elevation is mainly caused by reducing the imine–pyridine torsion angle of the Schiff base; the torsion angle is a principal factor that determines the Schiff base pK_a (*14*).

*To whom correspondence should be addressed. Tel: +81-726-84-6416, Fax: +81-726-84-6516, E-mail: med001@art.osaka-med.ac.jp

 © 2003 The Japanese Biochemical Society.

Downloaded from http://jb.oxfordjournals.org/ at Changhua Christian Hospital on September 29, 2012

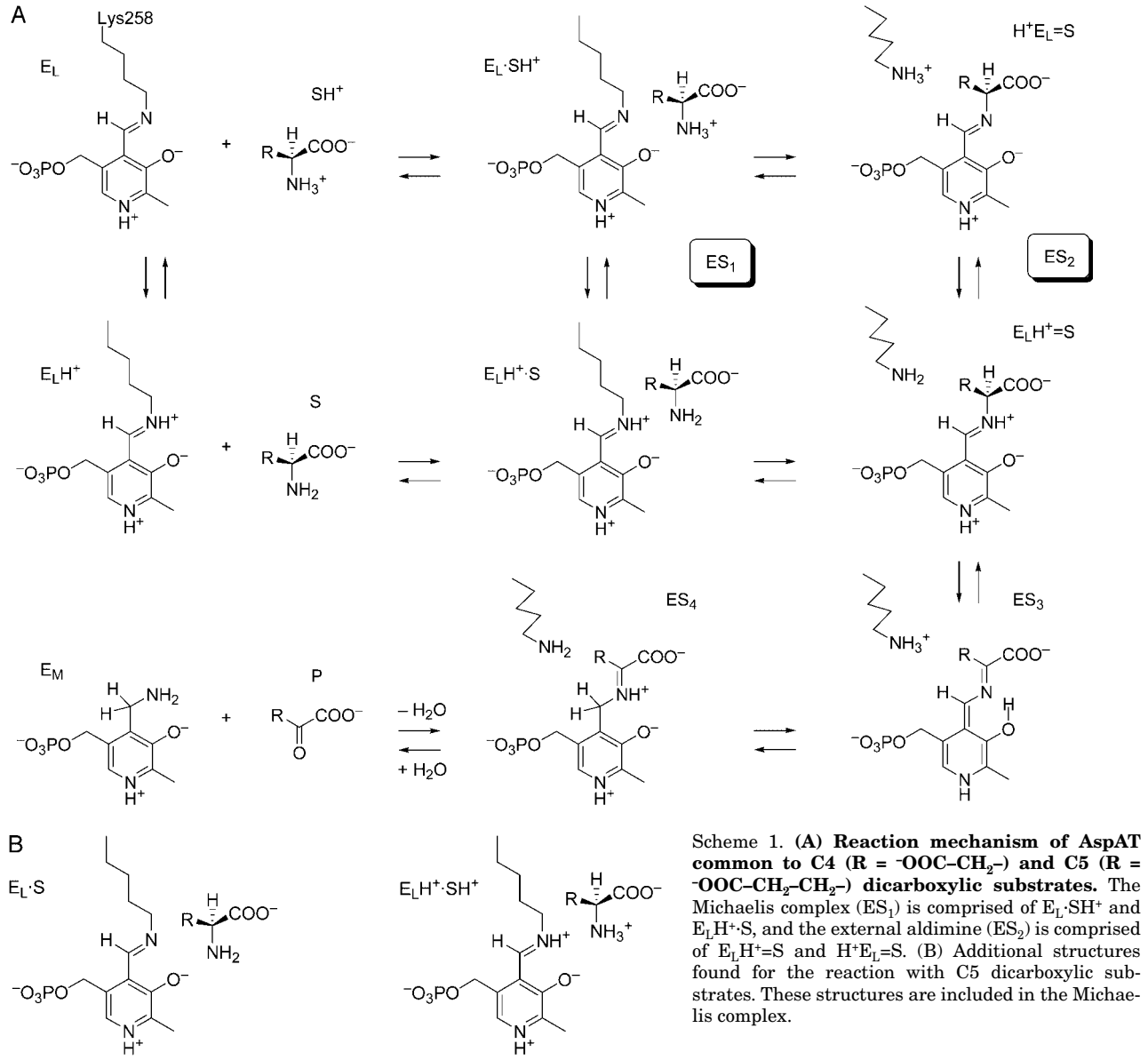

Scheme 1. **(A) Reaction mechanism of AspAT common to C4 (R = $^-$OOC–CH_2–) and C5 (R = $^-$OOC–CH_2–CH_2–) dicarboxylic substrates.** The Michaelis complex (ES_1) is comprised of $E_L{\cdot}SH^+$ and $E_LH^+{\cdot}S$, and the external aldimine (ES_2) is comprised of $E_LH^+{=}S$ and $H^+E_L{=}S$. (B) Additional structures found for the reaction with C5 dicarboxylic substrates. These structures are included in the Michaelis complex.

The C5 dicarboxylic substrates have the same terminal functional group as the C4 dicarboxylic substrates, and the two classes differ only in chain length. Therefore, it is anticipated that the reaction of the C5 substrates (Eq. 2) is similar to that of the C4 substrates (Eq. 1). However, owing to the larger K_d values of the C5 substrates and analogues (~10 times higher than the C4 counterparts), no detailed kinetic analysis of the reaction with C5 substrate has been carried out at present. In this study, we followed the spectral transition of AspAT on reaction with glutamate and found that the mechanism of the reaction at the early step of the catalysis differs significantly between the two classes of substrates.

EXPERIMENTAL PROCEDURES

Chemicals—*Escherichia coli* AspAT was obtained as described earlier (*17*) from *E. coli* JM103 cells containing pUC19–*aspC*. All other chemicals were of the highest grade commercially available.

Spectrophotometric Analysis—Absorption spectra were measured using a Hitachi U-3300 spectrophotometer at 298 K. The buffer solutions contained 50 mM buffer component(s) (PIPES, HEPES, or TAPS) with 0.1 M KCl and 1 mM EDTA. The concentration of the enzyme subunit was generally (*1–3*) × 10^{-5} M. The concentration of the AspAT subunit in solution was determined using the value ε_M = 47,000 M^{-1} cm^{-1} for the PLP form and ε_M = 46,000 M^{-1} cm^{-1} for the PMP form at 280 nm.

Kinetic Analysis—Stopped-flow spectrophotometry was performed using an Applied Photophysics (Leatherhead, UK) SX.17MV spectrophotometer at 298 K. The dead time was 2.3 ms under a pressure of 500 kPa. The program provided with the instrument was used for the analysis of exponential absorption changes. Time-resolved spectra were collected at 298 K using the SX.17MV system equipped with a photodiode array accessory and the XScan (Version 1.0) controlling software (Applied Photophysics).

Downloaded from http://jb.oxfordjournals.org/ at Changhua Christian Hospital on September 29, 2012

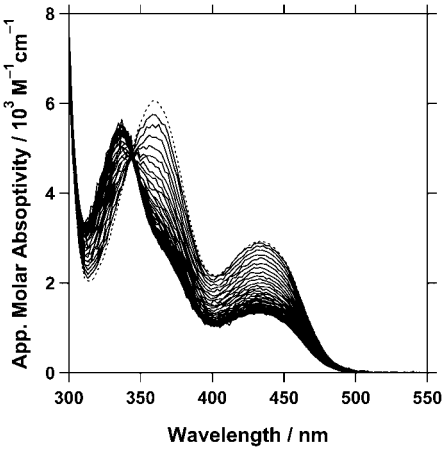

Fig. 1. **Time-dependent absorption changes of AspAT on reaction with glutamate at pH 7.0, 298K.** AspAT (38 μM) was reacted with 2 mM glutamate in PIPES-HEPES buffer, pH 7.0, in an Applied Photophysics SX.17MV stopped-flow spectrophotometer equipped with a photodiode array detector. The spectra were taken at 2.0 ms (flow stop), 3.84 ms, and then every 2.56 ms up to 254.72 ms. The initial spectrum is shown by a dotted line.

RESULTS

Spectral Change of AspAT on Reaction with Glutamate—At pH 7.0, AspAT has two absorption bands, at 430 nm and 358 nm (Fig. 1; dotted curve), which corresponds to the Schiff-base-protonated form (E_LH^+ in Scheme 1A) and the unprotonated form (E_L in Scheme 1A), respectively. On reaction with 2 mM glutamate, the two absorption bands at 358 nm and 430 nm decrease with concomitant increase in the absorption at 330 nm (Fig. 1), showing the formation of the PMP form of the enzyme (E_M in Scheme 1A). At various pH values, the decrease in absorbance at both 358 nm and at 430 nm follows a single exponential process (data not shown). The apparent rate constants, $k_{app,358}$ and $k_{app,430}$, respectively, are obtained and plotted against glutamate concentration (Fig. 2). The $k_{app,358}$ value shows an identical hyperbolic pattern for all pH values examined (6.0–7.0; Fig. 2A). On the other hand, the $k_{app,430}$ value is always smaller than the $k_{app,358}$ value, and the plots of $k_{app,430}$ shows different patterns with different pH values, the slope being steeper at higher pH values (Fig. 2B). These patterns are essentially identical to those observed for the reaction of AspAT with aspartate (*13*). In the case of the reaction with aspartate, the different behavior of $k_{app,430}$ and $k_{app,358}$ has been interpreted as being due to the slow rate of interconversion of the two ionic species of the PLP form of the enzyme, E_L and E_LH^+, compared to the transamination half reaction (*13*). Therefore, the observation with the reaction of AspAT with glutamate has tempted us to examine whether the reaction with glutamate can be analyzed in the same way as that with aspartate.

Considering the similarity to the reaction of AspAT with aspartate, we can draw the following scheme for the reaction of AspAT with glutamate:

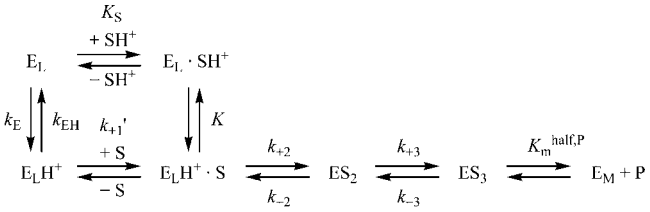

(Scheme 2)

S in Scheme 2 is the substrate amino acid with unprotonated α-amino group. The experiments were carried out at pH values below 7.0, where the majority of the substrate is in the form of SH^+. Therefore, we can assume a rapid equilibrium between $E_L + SH^+$, $E_L{\cdot}SH^+$, $E_LH^+{\cdot}S$, and ES_2. Accordingly, the reaction starting from the PLP form of AspAT to the PMP form can be reduced to the following mechanism, where E_{mix} stands for the mixture of E_L + SH^+, $E_L{\cdot}SH^+$, $E_LH^+{\cdot}S$, and ES_2:

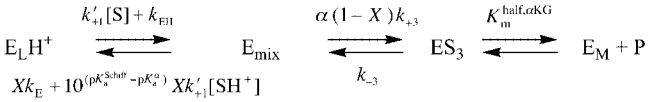

(Scheme 3)

where

$$X = \frac{(K_m^{half,\,Glu})_{alkaline}}{(K_m^{half,\,Glu})_{alkaline} + [SH^+]}$$

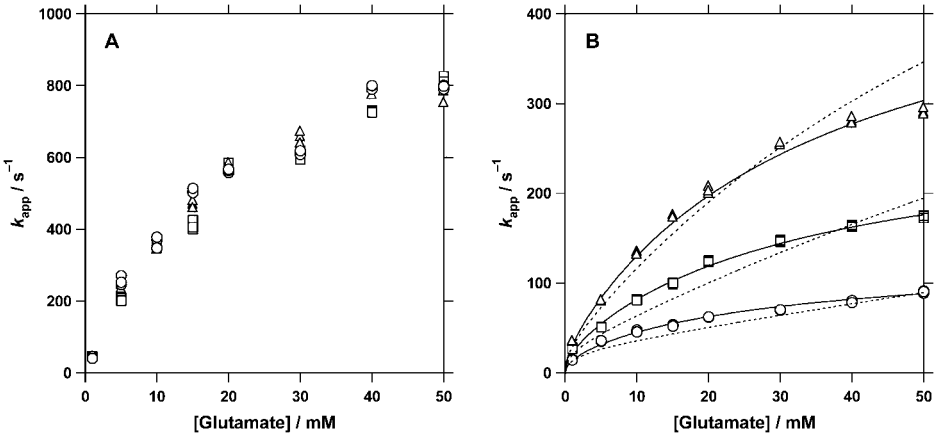

Fig. 2. **Dependency on the glutamate concentration and pH of the apparent rate constant for the spectral change.** AspAT (38 μM) was mixed with various buffers of different pH at various concentrations of glutamate at 298 K. (A) Plot of the k_{app} value for decrease in absorbance at 358 nm. Circles, pH 6.0; squares, pH 6.5; triangles, pH 7.0. (B) Plot of the k_{app} value for decrease in absorbance at 430 nm. Symbols are the same as those used in panel A. Three experimental values are plotted for a single concentration of glutamate, showing the reliability of the experiment.

Downloaded from http://jb.oxfordjournals.org/ at Changhua Christian Hospital on September 29, 2012

$$Y = \frac{2[\overline{\alpha KG}]}{K_m^{\text{half},\,\alpha KG} + 2[\overline{\alpha KG}]}$$

$$\alpha = \frac{K_{eq}^{\text{Glu}-\alpha KG}\,(K_m^{\text{half, Glu}})_{\text{alkaline}}}{K_m^{\text{half},\,\alpha KG}}\,\frac{k_{-3}}{k_{+3}}$$

$(K_m^{\text{half,Glu}})_{\text{alkaline}}$ is the alkaline-limiting value of the half-reaction k_m for glutamate and is expressed by the following equation:

$$(K_m^{\text{half, Glu}})_{\text{alkaline}} = \frac{k_{-1}}{k_{+1}} \cdot \frac{1}{1 + \left(1 + \frac{k_{+2}}{k_{-2}}\right)K} \qquad (5)$$

$[\overline{\alpha KG}]$ is the equilibrium concentration of 2-oxoglutarate. $K_{eq}^{\text{Glu}-\alpha KG}$ is the equilibrium constant for the half reaction and is related to the kinetic parameters in Scheme 2:

$$K_{eq}^{\text{Glu}-\alpha KG} = \frac{k_{+1}}{k_{-1}} \cdot K \cdot \frac{k_{+2}}{k_{-2}} \cdot \frac{k_{+3}}{k_{-3}} \cdot K_m^{\text{half},\,\alpha KG} \qquad (6)$$

The differential equations derived from this are easily solved to give the apparent rate constant as follows (*13*):

$$k_{\text{app},430} = \Big\{ L + M + \alpha(1-X)k_{+3} + Yk_{-3} - \sqrt{(L + M - \alpha(1-X)k_{+3} - Yk_{-3})^2 + 4M\alpha(1-X)k_{+3}} \Big\}/2 \qquad (7)$$

where

$$L = k'_{+1}[\text{S}] + k_{\text{EH}}$$

$$M = Xk_{\text{E}} + 10^{(\text{p}K_a^{\text{Schiff}} - \text{p}K_a^{\alpha})}Xk'_{+1}[\text{SH}^+]$$

We already know the values of the following kinetic parameters (*17*): $K_{eq}^{\text{Glu}-\alpha KG} = 0.040$, $(K_m^{\text{half,Glu}})_{\text{alkaline}} = 38$ mM, $K_m^{\text{half},\alpha KG} = 1.3$ mM, $\alpha k_{+3} = 800\ \text{s}^{-1}$ (equal to $k_{cat}^{\text{half.Glu}}$), and $k_{-1} = 600\ \text{s}^{-1}$. The values of k_E and k_{EH} are known from the pH-jump study to be 234 s^{-1} and 37.5 s^{-1} (pH 6.0), 101 s^{-1} and 46.6 s^{-1} (pH 6.5), 52.7 s^{-1} and 75.6 s^{-1} (pH 7.0), respectively. Therefore, theoretical lines can be drawn using Eq. 7, with k'_{+1} as the adjustable parameter. However, these lines do not fit the experimental data (Fig. 2B). The theoretical lines at the smallest root-mean-square deviation ($k'_{+1} = 1.4 \times 10^4\ \text{M}^{-1}\ \text{s}^{-1}$) are shown with dotted lines in Fig. 2B. All the lines show steeper slope than those based on the experimental data, *i.e.*, the theoretical values are smaller than the experimental data at low glutamate concentrations and larger at high glutamate concentrations. These deviations contrast sharply with the result for the reaction of AspAT with aspartate (*13*), in which the $k_{\text{app},430}$–pH plots fitted excellently to the equation equivalent to Eq. 7 with $k'_{+1} = 5.6 \times 10^6\ \text{M}^{-1}\ \text{s}^{-1}$. The present observation indicates that the reaction of AspAT with glutamate cannot be explained by Scheme 2.

We therefore sought other mechanism(s) that can explain the kinetic results of the reaction with glutamate. The experimental data show a tendency of saturation as compared to the theoretical lines derived from Scheme 2. That is, the $k_{\text{app},430}$ value is attenuated at higher glutamate concentration. In the case of the reaction of AspAT with aspartate, the increase in the $k_{\text{app},430}$ value with increasing concentration of aspartate or increasing pH is ascribed to the disappearance of E_LH^+ by association with S to form $E_LH^+{\cdot}S$ (*13*). Therefore, a mechanism in which the increased concentration of glutamate shrinks the flow of $E_LH^+ + S \rightarrow E_LH^+{\cdot}S$ would explain the experimental results. If we allow the association of SH^+, the major form of the substrate, with E_LH^+, to form a new species $E_LH^+{\cdot}SH^+$, the increase in the concentration of glutamate decreases the fraction of E_LH^+ in the ($E_LH^+/E_LH^+{\cdot}SH^+$) mixture, and decreases the apparent rate constant of conversion from ($E_LH^+/E_LH^+{\cdot}SH^+$) to E_{mix}.

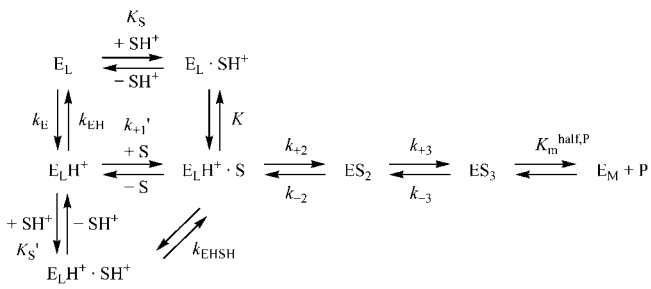

(Scheme 4)

Scheme 4 reduces to Scheme 5 in the same way that Scheme 2 reduces to Scheme 3:

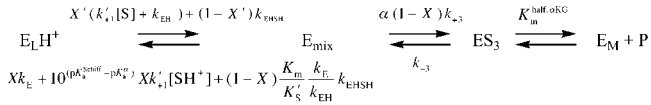

(Scheme 5)

where

$$X' = \frac{K'_S}{K'_S + [\text{SH}^+]}$$

The equation for $k_{\text{app},430}$ is identical to Eq. 7 except that L and M stand for the following combinations of terms:

$$L = X'(k'_{+1}[\text{S}]\ k_{\text{EH}}) + (1 - X')k_{\text{EHSH}}$$

$$M = Xk_{\text{E}} + 10^{(\text{p}K_a^{\text{Schiff}} - \text{p}K_a^{\alpha})}Xk'_{+1}[\text{SH}^+] + (1 - X)\frac{K_m}{K'_S}\frac{k_{\text{E}}}{k_{\text{EH}}}k_{\text{EHSH}}$$

The plots fit excellently to the equation as shown in Fig. 2B (solid lines), with $k'_{+1} = (2.3 \pm 0.2) \times 10^7\ \text{M}^{-1}\text{s}^{-1}$ and $K'_S = 35 \pm 2$ mM. As expected, the saturation at higher concentration of glutamate is properly reproduced. Thus, the incorporation of $E_LH^+{\cdot}SH^+$ into the scheme greatly improves the fitting. This is in clear contrast with the reaction of AspAT with aspartate, where the presence of $E_LH^+{\cdot}SH^+$ is not necessary for analyzing the reaction of AspAT and aspartate, and, therefore, the $E_LH^+{\cdot}SH^+$ species is considered to constitute only a negligible part of the Michaelis complex (*13*).

Fitting gives the value of $2.8 \times 10^{-14}\ \text{s}^{-1}$ (at pH 6) for k_{EHSH}. However, it has a large SD value of 1,800 s^{-1}. Actually, fixing k_{EHSH} at any particular value between 1 and 1,000 s^{-1} gives essentially the same fitting curves. Therefore, the present kinetic analysis cannot determine the rate of deprotonation of the α-amino group of glutamate in the $E_LH^+{\cdot}SH^+$ complex.

Downloaded from http://jb.oxfordjournals.org/ at Changhua Christian Hospital on September 29, 2012

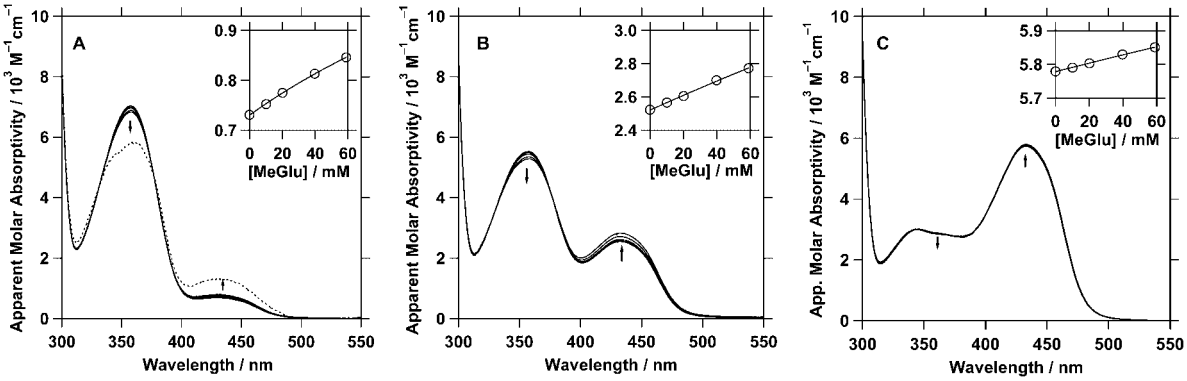

Fig. 3. **Spectral change of AspAT on binding of 2-methylglutamate.** AspAT (38 μM) was mixed with various concentrations of DL-2-methylglutamate, and the spectra were taken at 298 K. The concentration of 2-methylglutamate (L-form) is indicated in the inset, which shows the concentration dependency of the apparent molar absorptivity at 430 nm. The ordinate of the inset is the same as that of the spectral graph. (A) pH 8.1. Dotted line shows the spectrum of the AspAT–2-methylglutamate complex obtained by extrapolation of the spectra to the infinite concentration of 2-methylglutamate. The molar absorptivity at 430 nm is $(1.42 \pm 0.12) \times 10^3$ M^{-1} cm^{-1}. (B) pH 7.1. (C) pH 6.1. No saturation of the spectrum with increasing concentration of 2-methylglutamate is observed for (B) and (C).

Reaction of 2-Methylglutamate with AspAT—Substitution of a methyl group for the hydrogen at α-C of the amino acid substrate stops the catalytic reaction of aminotransferases at the step of the 1,3-prototropic shift (between ES_2 and ES_3 in Scheme 1A). Therefore, the two intermediates, the Michaelis complex and the external aldimine, are expected to accumulate on reaction of 2-methyl amino acids with aminotransferases. Analysis of the reaction of AspAT with 2-methylaspartate (MeAsp) led to successful resolution of the absorption spectra of the Michaelis complex and the external aldimine (*14*). Therefore, we analyzed the reaction of AspAT with 2-methylglutamate (MeGlu), in an attempt to characterize the Michaelis complex and the external aldimine of AspAT with the C5 dicarboxylate.

At pH 8.1, the binding of MeGlu to AspAT caused a slight increase in the absorption at 430 nm and a similarly slight decrease in the absorption at 358 nm (Fig. 3A). The magnitudes of the changes show hyperbolic dependency on the MeGlu concentration (Fig. 3A, inset). The direction of the spectral changes and the concentration dependency are the same as those observed for the reaction of AspAT with MeAsp (*14*). Extrapolation of the spectra to infinite concentration of MeGlu gave the spectrum shown by the dotted line in Fig. 3A. The spectrum has a large peak at around 360 nm with a smaller one at 430 nm, indicating that the Schiff base of the AspAT–MeGlu complex is preferentially unprotonated at pH 8.1. Binding of MeGlu to AspAT at pH 7.1 and pH 6.1 causes a similar tendency in the spectral changes. The changes at pH 7.1 are more apparent than the changes at pH 8.1, but showed essentially no saturation with increasing glutamate concentration. Accordingly, it is difficult to obtain the spectra of the AspAT–MeGlu complex by extrapolation to infinite concentration of MeGlu at these pH values. However, the magnitudes of the spectral changes strongly suggest that the Schiff base of the AspAT–MeGlu complex is largely protonated at pH 7.1 and 6.1.

Binding of Glutarate to AspAT—Glutarate is a desamino analogue of glutamate, and owing to this chemical property, it is expected to form a complex with AspAT but not to proceed to the external aldimine (blocked at the step $ES_1 \rightarrow ES_2$ in Scheme 1A). Therefore, the AspAT–glutarate complex can be considered to be a model for the Michaelis complex. On binding of glutarate to AspAT, the 430-nm absorption of the enzyme increases with concomitant decrease in the 358-nm absorption. As the 430-nm and 358-nm absorption bands reflect the protonated and unprotonated forms of the PLP–Lys258 Schiff base, respectively, the spectral changes indicate that the glutarate binding increases the pK_a of the Schiff base. At a fixed pH value, the spectral changes show a hyperbolic dependency on the glutarate concentration, and extrapolation to infinite concentration of glutarate yields the spectrum of the AspAT–glutarate complex at that pH. The spectra are obtained for several pH values, and the 430-nm absorption was plotted against the solution pH (Fig. 4). Fitting of the plots to Eq. 8, in which e_E and e_{EH} represent the molar extinction coefficients of E_L and E_LH^+, respectively, yields the pK_a of the Schiff base of the AspAT–glutarate complex, and the value is determined to be 8.1, which is 1.3 unit higher than that of the unliganded AspAT.

$$\varepsilon_{app} = \varepsilon_E + \frac{\varepsilon_{EH} - \varepsilon_E}{1 + 10^{pH - pK_a}} \quad (8)$$

The value is 0.7 unit lower than the value for the AspAT–maleate complex, indicating that the C5-dicarboxylate increases the basicity of the Schiff base, but its effect is weaker than that of the C4-dicarboxylate.

DISCUSSION

Multiple Substrate-Binding Process—The binding of aspartate to AspAT occurs via two distinct routes, the association of E_L and SH^+, and that of E_LH^+ and S (*13*). This mechanism is also applicable to the reaction of aromatic amino acid aminotransferase (ArAT) with aspartate and phenylalanine (*18*). The present study shows that the reaction of AspAT with glutamate involves this dual substrate-binding mechanism, and that the mechanism is common to the association process of amino acid substrates and AspAT-family enzymes, in which the

Downloaded from http://jb.oxfordjournals.org/ at Changhua Christian Hospital on September 29, 2012

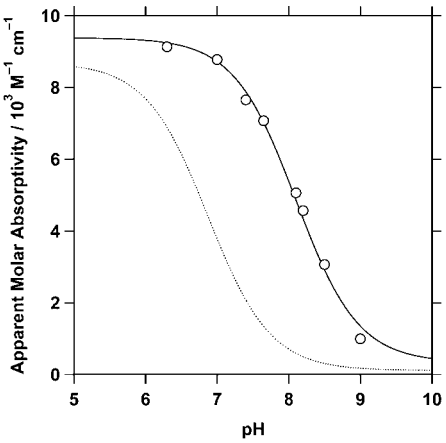

Fig. 4. **pH dependency of the apparent molar absorptivity at 430 nm of the AspAT–glutarate complex.** The spectrum of the AspAT–glutarate complex was obtained by extrapolating the spectra of AspAT in the presence of glutarate at a fixed pH to infinite concentration of glutarate. The apparent molar absorptivity at 430 nm is plotted against pH. A theoretical line is drawn using Eq. 8. ε_E is set to 0 because the unprotonated PLP Schiff base has no absorption over 400 nm. For comparison, the corresponding line of AspAT in the absence of glutarate is shown by a dotted line.

PLP–Lys Schiff base exists both in the protonated and unprotonated forms. The association rate constant for E_LH^+ and S is 5.1×10^6 M^{-1} s^{-1} for AspAT and aspartate (*13*), 1.2×10^7 M^{-1} s^{-1} for ArAT and phenylalanine (*18*), and 2.3×10^7 M^{-1} s^{-1} for AspAT and glutamate (this study). Thus, all are of the same order irrespective of the combination of the substrate and enzyme, indicating that the affinity of the substrate and enzyme is determined by the rate of dissociation rather than the rate of association. The present study, however, also shows that the reaction of AspAT with glutamate involves association of E_LH^+ and SH^+, a new route which has not been found for the reaction of AspAT with aspartate or ArAT with aspartate and phenylalanine. The association of E_LH^+ and SH^+ yields a new protonation species $E_LH^+{\cdot}SH^+$ in the Michaelis complex, which is discussed in the next section.

Protonation Status in the Michaelis complex—The pattern of the spectral change on binding of MeGlu to AspAT differs strikingly from that of MeAsp. The AspAT–MeAsp complex shows a spectrum essentially independent of the solution pH (*14*). This is because both the Michaelis complex and the external aldimine contain only species which have same number of protons (see introduction), *i.e.*, a proton shuttles between the Schiff base N and the amino N of the substrate (Michaelis complex) or Lys258 (external aldimine). The observation that the AspAT–MeGlu complex shows apparent dependency on pH (Fig. 3) indicates that the "proton-shuttling mechanism" observed for the AspAT–MeAsp complex does not apply to the AspAT–MeGlu complex. This is consistent with the mechanism of Scheme 3, in which the species $E_LH^+{\cdot}SH^+$, which has one more proton than $E_L{\cdot}SH^+$ and $E_LH^+{\cdot}S$ (the components of the proton-shuttling mechanism), is taken into account. It is, therefore, important to determine whether the pH dependency of the spectrum of the AspAT–MeGlu complex can be explained by Scheme 3.

The complicated protonation states of the Michaelis complex of AspAT and glutamate can be understood by considering the three-dimensional free energy profile (Fig. 5). The relative height of the individual energy levels is calculated as follows. The pK_a of the α-amino group of glutamate bound to E_LH^+ is:

$$pK_a^{EH,\alpha} = pK_a^{Schiff} + \log\left(\frac{K_m}{K'_S}\frac{1+K}{K}\right) \quad (9)$$

The K value is estimated to be ~10 by global spectral analysis of the reaction of AspAT with glutamate (Hayashi et al., unpublished results). Using the K'_S and K_m values described above, the $pK_a^{EH,\alpha}$ value is calculated to be 6.8. From this pK_a value the free-energy difference between $E_LH^+{\cdot}S$ and $E_LH^+{\cdot}SH^+$ is calculated. The energy difference between $E_LH^+{\cdot}S$ and $E_L{\cdot}SH^+$ is determined by K. The energy difference between $E_L{\cdot}S$ and $E_LH^+{\cdot}S$ is derived from the pK_a value of the Schiff base when S is bound to the active site. Since S has no positive charge at the α-amino group, we can expect that the electrostatic contribution of S is similar to that of glutarate. Therefore, we used the value of pK_a = 8.1 for the estimation. The energy profiles at pH 8.1 (Fig. 5A) and 7.1 (Fig. 5B) are shown.

At pH 8.1, both $E_L{\cdot}S$ and $E_LH^+{\cdot}S$ have the identical, lowest energy level in the Michaelis complex. Therefore, the Schiff base of the Michaelis complex (ES_1) is 50% protonated at pH 8.1. At pH 7.1, $E_LH^+{\cdot}S$ has the lowest energy level, and $E_LH^+{\cdot}SH^+$ has a slightly higher energy level in the Michaelis complex. That is, the Schiff base is almost completely protonated at pH 7.1. Assuming that the external aldimine has a pH-independent spectrum (refer to the discussion in the last section), the energy profile can explain the observed spectral changes on binding of MeGlu to AspAT as follows. At pH 8.1, the free enzyme exists almost exclusively as E_L. The MeGlu binding would yield $E_L{\cdot}S$ and $E_LH^+{\cdot}S$ in equal amounts. At pH 7.1, the free enzyme exists as both E_L and E_LH^+. The binding of MeGlu would yield $E_LH^+{\cdot}S$ and $E_LH^+{\cdot}SH^+$, both of which have a protonated Schiff base. Therefore, the MeGlu binding increases the 430-nm absorption band at both pH 8.1 and 7.1. At pH 6.1, $E_LH^+ + SH^+$ and $E_LH^+{\cdot}SH^+$ have the lowest energy level in the starting state ("Free" in Fig. 5) and the Michaelis complex ("ES_1" in Fig. 5), respectively. Therefore, the Schiff base is almost completely protonated at both steps. Accordingly, the binding of MeGlu does not significantly change the spectrum at pH 6.1 (Fig. 3).

The relative height of the energy levels in the Michaelis complex provides important information on the structure of the Michaelis complex. The increase in energy from $E_L{\cdot}SH^+$ to $E_LH^+{\cdot}SH^+$ is only 1.7 kJ mol^{-1} larger than that from $E_L{\cdot}S$ to $E_LH^+{\cdot}S$ (Fig. 5). Therefore, the protonation of the α-amino group of glutamate does not significantly attenuate the protonation of the Schiff base in the Michaelis complex. This strongly indicates that there is essentially no interaction between the Schiff base and the α-amino group of glutamate in the Michaelis complex.

Structural Basis—The above observations with C5 dicarboxylates are in sharp contrast with the corresponding results with the C4-dicarboxylates, which show that only $E_LH^+{\cdot}S$ and $E_L{\cdot}SH^+$ exist in the Michaelis complex. The crystal structure of AspAT complexed with maleate

Downloaded from http://jb.oxfordjournals.org/ at Changhua Christian Hospital on September 29, 2012

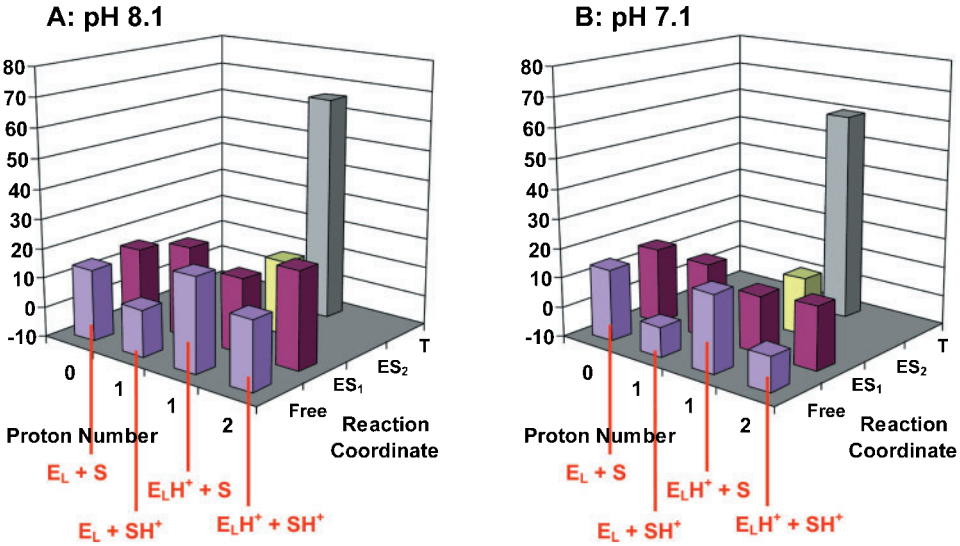

Fig. 5. **Free energy diagram for the reaction of AspAT with glutamate at pH 8.1 (A) and pH 7.1 (B).** The energy levels of the intermediates were calculated from the equilibrium constants (see text for detail). Free, starting state (unliganded enzyme plus substrate); ES_1, Michaelis complex; ES_2, external aldimine; T, transition state for the half reaction. The equilibrium constant between the Michaelis complex and the external aldimine was set to 1 (*5*). The activation free energy starting from the ES_1/ ES_2 mixture to T was calculated from $k_{cat}^{half,Glu}$ = 800 s^{-1}. The components of ES_1 are, from left to right, $E_L{\cdot}S$, $E_L{\cdot}SH^+$, $E_LH^+{\cdot}S$, and $E_LH^+{\cdot}SH^+$.

indicates that, if aspartate is modeled on the bound maleate, the α-amino group points toward the imine of the Schiff base (Fig. 6A). If both N atoms are protonated, there is a strong electrostatic repulsion between the two groups. Alternatively, if both N atoms are unprotonated, the lone pair electrons will cause electrostatic repulsion. Thus, the structure with a single proton shared by the two N atoms, i.e., the mixture of $E_L{\cdot}SH^+$ and $E_LH^+{\cdot}S$, is stable, and these two species are dominant irrespective of pH [proton-shuttling mechanism (*14*)].

Based on this mechanism, we are interested in the distance between the amino and the imino N atoms in the Michaelis complex with glutamate. Unfortunately, models for the Michaelis complex of AspAT and glutamate, such as the glutarate complex of the PLP form of AspAT, have not been obtained so far. However, Malashkevich *et al.* have carried out detailed crystallographic and spectroscopic analysis on the glutamate complex of chicken mitochondrial AspAT that gives insights into the structure of the Michaelis complex with glutamate (*5*). From spectroscopic analysis, they showed that the Michaelis complex/external aldimine equilibrium differs greatly between when the enzyme in crystal and in solution. As the crystal packing force is expected to fix the conformation to the closed form, whereas the force is liberated when AspAT is in solution, the result suggests that the Michaelis complex and the external aldimine take different conformations. Additionally, the structure of the complexes of the PMP form of AspAT with maleate and glutarate give important information (*9*) (shown in modified form in Fig. 6B). The maleate complex is in the closed conformation, in which the small domain approaches the large domain. Maleate forms strong hydrogen bonds with Arg292* and Arg386, and the position and the conformation of maleate are essentially identical to those of maleate in the PLP form of AspAT (*7*). On the other hand, the enzyme protein of the glutarate complex is in the open form, which is superimposable onto that of the unliganded enzyme (*9*). One of the carboxylate groups of glutarate forms bifurcated hydrogen bonds with the guanidinium group of Arg386, but the hydrogen bonds are elongated because, in the open conformation, Arg386, located in the small domain, does not approach the ligand. The other carboxylate group of glutarate does not form the bifurcated hydrogen bonds with Arg292* and is located between Tyr70* and Arg292*, suggesting weak interactions with these residues. As a result, the conformation of Cβ–Cα–C (carboxylate) is twisted by almost 180 from that of maleate. Accordingly, the position of Cα (carbon atom next to the carboxylate group bound to Arg386) is away from the Schiff base by about 2.1 Å. Furthermore, if we attach an amino group to Cα of glutarate to form L-glutamate, the amino group is pointed toward the solvent side, which is opposite to the Schiff base (Fig. 6B). Therefore, if glutamate of the Michaelis complex takes the same conformation as that shown in Fig. 6B, the α-amino group is expected to be far away from the imino group of the Schiff base. The assumed weak interaction between the two groups explains clearly why $E_L{\cdot}S$ and $E_LH^+{\cdot}SH^+$ are allowed to exist as components of the Michaelis complex.

Another important thing to note is that the lower Schiff base pK_a value of the C5-dicarboxylate liganded AspAT as compared to the C4-dicarboxylate liganded AspAT can be understood by the conformational difference of the enzyme protein. The increase in the Schiff base pK_a on the binding of C4-dicarboxylates (maleate or succinate) is around 2 pH unit, and 0.7 unit is ascribed to the destabilization of the unprotonated PLP–Lys258 Schiff base by the unfavorable interaction of the Schiff base, the Tyr225 side chain, and the Gly38 main chain, which is induced by the open-to-closed conformational change of AspAT on the C4-dicarboxylate binding (*16*). As this conformational change does not occur on the C5-dicarboxylate binding to AspAT, the increase in the Schiff base pK_a on C5-dicarboxylate binding is expected to be lower than that on C4-dicarboxylate binding by 0.7 unit, which is consistent with the experimental finding (Fig. 5).

Recognition of C5 and C4 Substrates—Previous crystallographic analyses (*3*, *4*, *6–8*) showed that the C4 dicarboxylates are accommodated to AspAT as follows. The α- and β-carboxylate groups form strong bifurcated hydrogen bonds with Arg386 and Arg292*, respectively. When the AspAT protein takes the closed conformation,

Downloaded from http://jb.oxfordjournals.org/ at Changhua Christian Hospital on September 29, 2012

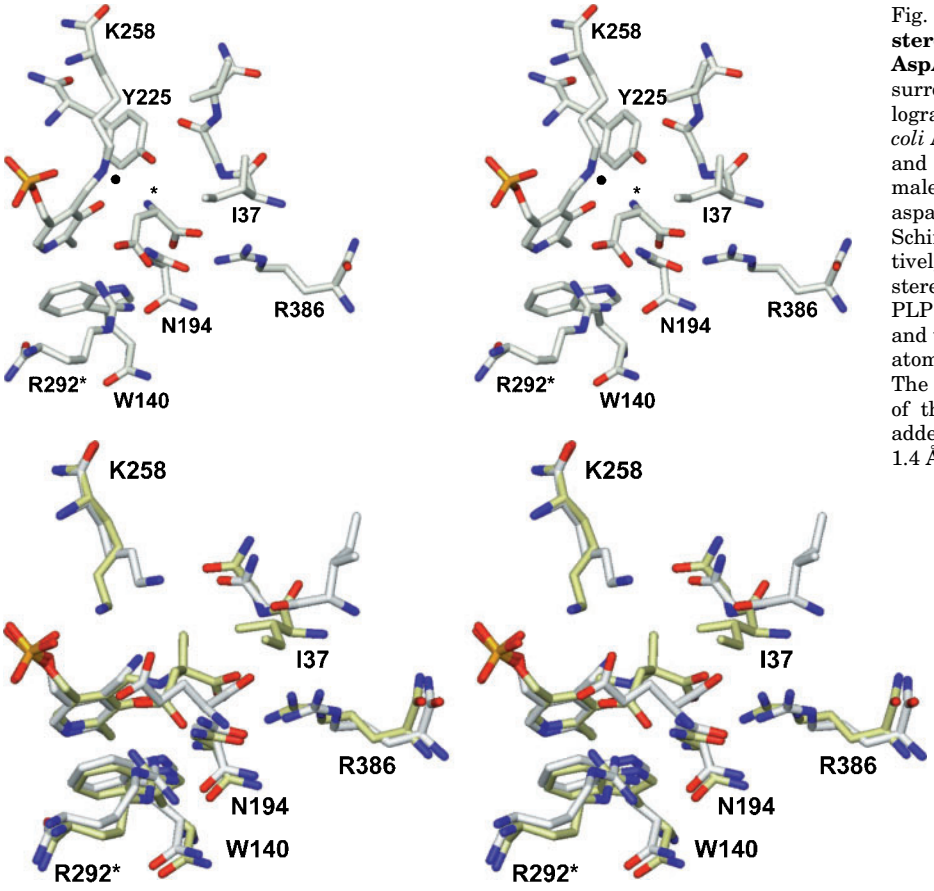

Fig. 6. **(A) Proposed structure (parallel stereo view) of the Michaelis complex of AspAT with aspartate.** The ligand and the surrounding residues are shown. The crystallographic structure of the maleate-bound *E. coli* AspAT [1ASM (*7*)] was used as the model, and an amino group was added to Cα of maleate (C–N distance to be 1.4 Å) to form L-aspartate. The substrate–amino N and the Schiff-base N are indicated by * and •, respectively. (B) Superimposed structures (parallel stereo view) of the 2-methylaspartae–bound PLP form [carbon atoms in khaki; 1ART (*8*)], and the glutarate-liganded PMP-form [carbon atoms in white; 1AMQ (*9*)] of *E. coli* AspAT. The structures were aligned at the Cα atoms of the large domain. An amino group was added to Cα of glutarate (C–N distance to be 1.4 Å) to form L-glutamate.

the position of Arg386, located in the small domain, and that of Arg292*, located in the large domain, are ideal for accommodating the energetically favorable *gauche* conformation of the C4 dicarboxylates. Accordingly, the AspAT–C4 dicarboxylate complex takes the closed conformation both in the Michaelis complex and the external aldimine.

The structure of the ketimine complex of glutamate of chicken mitochondrial AspAT (*5*) shows how the C5 substrate is accommodated in the closed form of the enzyme. The positions of the α-carboxylate group and Arg386, and the positions of the distal carboxylate group and Arg292*, are superimposable onto those of the complex of AspAT with C4 analogues (*e.g.*, maleate and 2-methylaspartate). As a result, the β and γ methylene groups are forced to reside in the space between Cα and the distal carboxylate group. Cγ is, therefore, displaced from the Cβ–γ-carboxylate line and causes steric hindrance with Ile37 and Tyr70*. This unfavorable puckering of the Cβ–Cγ chain of the C5 dicarboxylates causes a force to be applied to move Cα and α-carboxylate toward the small domain (schematically shown in Fig. 7). In the Michaelis complex, there is no covalent bond between Cα and the coenzyme PLP. Therefore, the force applied to Cα and α-carboxylate would cause opening of the interface between the small and large domains, resulting in the stretched conformation of the C5-dicarboxylate in the open form of the enzyme, which is found for the glutarate complex of the PMP form of AspAT (*9*). This structure is the basis for the pH-dependent multiple protonation state of the Michaelis complex as discussed in the previous section. On the other hand, if there is a covalent bond between Cα and the coenzyme (Fig. 7, right), the position of Cα is fixed, and AspAT can take a closed conformation, which is actually observed for the ketimine complex of glutamate (*5*). Therefore, we can expect that the external aldimine of AspAT with glutamate (or MeGlu) has essentially a similar conformation to that of AspAT with aspartate (or MeAsp). Accordingly, the β-amino group of Lys258 is expected to be close to the imino group of the

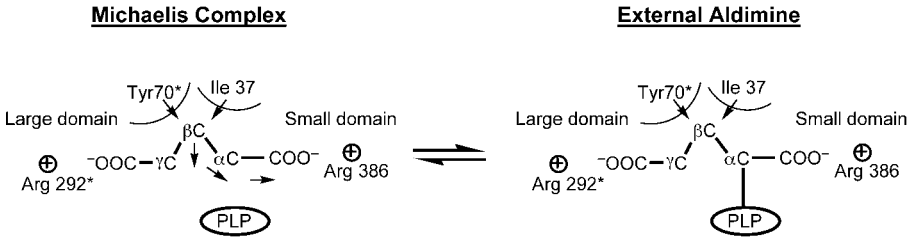

Fig. 7. **Schematic diagram showing how the puckering of the Cβ–Cγ chain of the C5 dicarboxylates pushes Cα toward the small domain.** See text for details.

Downloaded from http://jb.oxfordjournals.org/ at Changhua Christian Hospital on September 29, 2012

PLP–substrate Schiff base and a proton is shared by the two groups, providing a pH-independent protonation state of the external aldimine.

Aminotransferases transfer amino group between two substrates, and, therefore, recognize two or more substrates that differ in the skeleton. Aromatic amino acid aminotransferase recognizes the carboxylic side chain (aspartate) and aromatic side chain (phenylalanine and tyrosine) at the same site of the enzyme protein (*19*, *20*). The recognition of the two classes of substrates with different properties (acidic and aromatic) is carried out by reorganization of the hydrogen-bond network in the enzyme from *Paracoccus denitrificans* (*21*), or switching of the side chain of Arg292* in the enzyme from *Escherichia coli* (*20*). All these enzyme–substrate complexes are in the closed form. The present kinetic study strongly supports the idea that the Michaelis complex of the C5-dicarboxylate complex of AspAT takes an open conformation to avoid puckering the side chain of the C5-dicarboxylate. Thus, AspAT recognizes substrates with different chain lengths by changing the gross conformation of the enzyme protein. This mechanism of multiple substrate recognition is a novel one, and it is interesting to explore the catalytic significance of the mechanism, which is now under way in our laboratory.

This work was supported in part by a grant fo Scientific Research on Priority Areas (No. 13125101 to H.H.), and a Grant-in-Aid for Scientific Research (No. 13680697 to H.H.) from the Japan Society for the Promotion of Science. Amino acid residues are numbered according to the sequence of pig cytosolic aspartate aminotransferase (*1*). An asterisk indicates that the residue comes from the neighboring subunit.

REFERENCES

1. Ovchinnikov, Y.A., Egorov, C.A., Aldanova, N.A., Feigina, M.Y., Lipkin, V.M., Abdulaev, N.G., Grishin, E.V., Kiselev, A.P., Modyanov, N.N., Braunstein, A.E., Polyanovsky, O.L., and Nosikov, V.V. (1973) The complete amino acid sequence of cytoplasmic aspartate aminotransferase from pig heart. *FEBS Lett.* **29**, 31–34
2. Kiick, D.M. and Cook, P.F. (1983) pH studies toward the elucidation of the auxiliary catalyst for pig heart aspartate aminotransferase. *Biochemistry* **22**, 375–382
3. Rhee, S., Silva, M.M., Hyde, C.C., Rogers, P.H., Metzler, C.M., Metzler, D.E., and Arnone, A. (1997) Refinement and comparisons of the crystal structures of pig cytosolic aspartate aminotransferase and its complex with 2-methylaspartate. *J. Biol. Chem.* **272**, 17293–17302
4. McPhalen, C.A., Vincent, M.G., Picot, D., Jansonius, J.N., Lesk, A.M., and Chothia, C. (1992) Domain closure in mitochondrial aspartate aminotransferase. *J. Mol. Biol.* **227**, 197–213
5. Malashkevich, V.N., Toney, M.D., and Jansonius, J.N. (1993) Crystal structures of true enzymatic reaction intermediates: aspartate and glutamate ketimines in aspartate aminotransferase. *Biochemistry* **32**, 13451–13462
6. Jäger, J., Pauptit, R.A., Sauder, U., and Jansonius, J.N. (1994) Three-dimensional structure of a mutant *E. coli* aspartate aminotransferase with increased enzymic activity. *Protein Eng.* **7**, 605–612
7. Jäger, J., Moser, M., Sauder, U., and Jansonius, J.N. (1994) Crystal structures of *Escherichia coli* aspartate aminotransferase in two conformations. Comparison of an unliganded open and two liganded closed forms. *J. Mol. Biol.* **239**, 285–305
8. Okamoto, A., Higuchi, T., Hirotsu, K., Kuramitsu, S., and Kagamiyama, H. (1994) X-ray crystallographic study of pyridoxal 5′-phosphate-type aspartate aminotransferases from *Escherichia coli* in open and closed form. *J. Biochem.* **116**, 95–107
9. Miyahara, I., Hirotsu, K., Hayashi, H., and Kagamiyama, H. (1994) X-ray crystallographic study of pyridoxamine 5′-phosphate-type aspartate aminotransferases from *Escherichia coli* in three forms. *J. Biochem.* **116**, 1001–1012
10. Kirsch, J.F., Eichele, G., Ford, G.C., Vincent, M.G., Jansonius, J.N., Gehring, H., and Christen, P. (1984) Mechanism of action of aspartate aminotransferase proposed on the basis of its spatial structure. *J. Mol. Biol.* **174**, 497–525
11. Goldberg, J.M. and Kirsch, J.F. (1996) The reaction catalyzed by *Escherichia coli* aspartate aminotransferase has multiple partially rate-determining steps, while that catalyzed by the Y225F mutant is dominated by ketimine hydrolysis. *Biochemistry* **35**, 5280–5291
12. Toney, M.D. and Kirsch, J.F. (1993) Lysine 258 in aspartate aminotransferase: enforcer of the Circe effect for amino acid substrates and general-base catalyst for the 1, 3-prototropic shift. *Biochemistry* **32**, 1471–1479
13. Hayashi, H. and Kagamiyama, H. (1997) Transient-state kinetics of the reaction of aspartate aminotransferase with aspartate at low pH reveals dual routes in the enzyme-substrate association process. *Biochemistry* **36**, 13558–13569
14. Hayashi, H., Mizuguchi, H., and Kagamiyama, H. (1998) The imine–pyridine torsion of the pyridoxal 5′-phosphate Schiff base of aspartate aminotransferase lowers its pK_a in the unliganded enzyme and is crucial for the successive increase in the pK_a during catalysis. *Biochemistry* **37**, 15076–15085
15. Mizuguchi, H., Hayashi, H., Okada, K., Miyahara, I., Hirotsu, K., and Kagamiyama, H. (2001) Strain is more important than electrostatic interaction in controlling the pK_a of the catalytic group in aspartate aminotransferase. *Biochemistry* **40**, 353–360
16. Hayashi, H., Mizuguchi, H., Miyahara, I., Nakajima, Y., Hirotsu, K., and Kagamiyama, H. (2003) Conformational change in aspartate aminotransferase on substrate binding induces strain in the catalytic group and enhances catalysis. *J. Biol. Chem.* **278**, 9481–9488
17. Kuramitsu, S., Hiromi, K., Hayashi, H., Morino, Y., and Kagamiyama, H. (1990) Pre-steady-state kinetics of *Escherichia coli* aspartate aminotransferase catalyzed reactions and thermodynamic aspects of its substrate specificity. *Biochemistry* **29**, 5469–5476
18. Islam, M.M., Hayashi, H., Mizuguchi, H., and Kagamiyama, H. (2000) The substrate activation process in the catalytic reaction of *Escherichia coli* aromatic amino acid aminotransferase. *Biochemistry* **39**, 15418–15428
19. Hayashi, H., Inoue, K., Mizuguchi, H., and Kagamiyama, H. (1996) Analysis of the substrate-recognition mode of aromatic amino acid aminotransferase by combined use of quasisubstrates and site-directed mutagenesis: systematic hydroxy-group addition/deletion studies to probe the enzyme-substrate interactions. *Biochemistry* **35**, 6754–6761
20. Malashkevich, V.N., Onuffer, J.J., Kirsch, J.F., and Jansonius, J.N. (1995) Alternating arginine-modulated substrate specificity in an engineered tyrosine aminotransferase. *Nat. Struct. Biol.* **2**, 548–553
21. Okamoto, A., Nakai, Y., Hayashi, H., Hirotsu, K., and Kagamiyama, H. (1998) Crystal structures of *Paracoccus denitrificans* aromatic amino acid aminotransferase: a substrate recognition site constructed by rearrangement of hydrogen bond network. *J. Mol. Biol.* **280**, 443–461

Downloaded from http://jb.oxfordjournals.org/ at Changhua Christian Hospital on September 29, 2012